Observation of Electric Quadrupole Decay in Xe^{45+} and Xe^{44+}

D. D. Dietrich, G. A. Chandler, R. J. Fortner, C. J. Hailey,[a] and R. E. Stewart
University of California, Lawrence Livermore National Laboratory, Livermore, California 94550
(Received 19 November 1984)

We have observed, for the first time in highly ionized atoms, electric quadrupole transitions between the $3p$ and $2p$ levels of fluorinelike and neonlike Xe^{45+} and Xe^{44+}. We have made precision measurements ($\lambda/\Delta\lambda = 2\times 10^4$) of the relative wavelengths of the allowed electric dipole ($E1$) transitions and the forbidden electric quadrupole ($E2$) transitions connecting the $n=3$ and the $n=2$ levels. We have also derived from these measurements several $\Delta n = 0$ intervals between states of opposite parity.

PACS numbers: 32.30.Rj, 31.30.Jv, 35.80.+s

In this Letter we report the first observations of the electric quadrupole transitions connecting the $3p$ to the $2p$ states in the fluorinelike and neonlike isoelectronic sequences. These observations establish fine-structure intervals between levels of opposite parity in a regime not previously accessible and also introduce the possibility of measuring the decay rates directly. These observations allow spectroscopic identification of $3\rightarrow 3$ transitions of interest in recent extreme-ultraviolet laser experiments[1] in a straightforward manner.

Recent experiments[2-6] on intrashell transitions near the closed l shell have been limited to ions with a moderate nuclear charge ($Z=39$ for F-like, $Z=28$ for Ne-like, and $Z=42$ for Na-like). Paralleling these experiments are improvements in both *ab initio*[7] and semiempirical calculations.[8,9] In the spectral region of the $3\rightarrow 3$ transitions, the experimentally observed density of lines increases dramatically over that of the $2\rightarrow 2$ region because of the increase in the numbers of levels, especially in the presence of adjacent charge states belonging to the Mg, Al, and Si isoelectronic sequences. There is also an increase in the variation in the results for predicted wavelengths among the several *ab initio* calculations[10-13] commonly used today. These theoretical variations are caused by difficulties in obtaining accurate relativistic multiconfigurational wave functions due to the increasing importance of multielectron relativistic and quantum electrodynamic effects. These difficulties can lead to errors of a few percent in the intrashell transition energies making identifications of observed lines very uncertain, if not impossible, far from the existing established isoelectronic sequences. The same errors represent a one-part-in-a-thousand uncertainty in the calculation of $n=3$ to $n=2$ intervals. The result is that unambiguous identifications can be made for these x-ray transitions by comparing our results (absolute uncertainty of 1:1500) with *ab initio* calculations.[13] The current results at $Z=54$ represent an application of this technique far beyond existing data used to establish isoelectronic sequences.

Previous studies of forbidden transitions in highly ionized systems[14] have centered on the $n=2$ to $n=1$ radiation from ions isoelectronic with hydrogen and helium, where there is no electric quadrupole radiation. In 1927, Bowen[15] first identified several prominent lines in the spectra of *galactic nebulae* as transitions between levels belonging to the normal configurations of various atoms and ions that had previously been conjectured as transitions in an extraterrestial element "nebulium." Since then, much work has been done both theoretically[16] and experimentally[17] on intrashell forbidden transitions. It should be noted that for these $\Delta n = 0$ transitions the $M1$ rates tend to be several orders of magnitude larger than the $E2$ rates.[16] Rates for transitions involving a change in principle quantum number have been calculated for over twenty years[18,19] but measurements have been limited to neutrals and near neutrals where rates of 10^2 sec^{-1} are large.[20]

The Grotrian diagram, Fig. 1(a), for neonlike Xe shows the sixteen levels of the $1s^22s^22p^53s$, $3p$, and $3d$ configurations with the $J=\frac{3}{2}$ core. Also indicated are the calculated decay rates for the observed and competing transitions in the present experiment. The transitions from the $3s$ and $3d$ to the $1s^22s^22p^6$ ground state are allowed electric dipole transitions, while the ones from the $3p$ to the ground state are electric quadrupole. Not seen in the present experiment are the $M1$ or $M2$ decays indicated by the dashed lines in Fig. 1(a). This is because the decay rates [see Fig. 1(a)] are too small for us to observe. In a previous observation[21] of these $E1$ transitions in a laser-produced plasma, electric quadrupole lines were not seen because of the high densities involved in that experiment. Lower-Z Ne-like ions have been studied with the beam-foil method,[22] and the $E2$ transitions were not seen because the allowed intrasystem $3p$-$3s$ transition rate dominates the $3p$-$2p$ $E2$ rates as shown in Fig. 1(b). Also shown in Fig. 1(b) is the magnetic dipole rate from the nearest $J=1$ $3p$ level. The $E1$ rates scale approximately linearly with Z while the $E2$ and $M1$ rates scale approximately as Z^6.

A description and schematic diagram of the apparatus used in this work have been presented previously[23] and will be reviewed only briefly here. Ions of

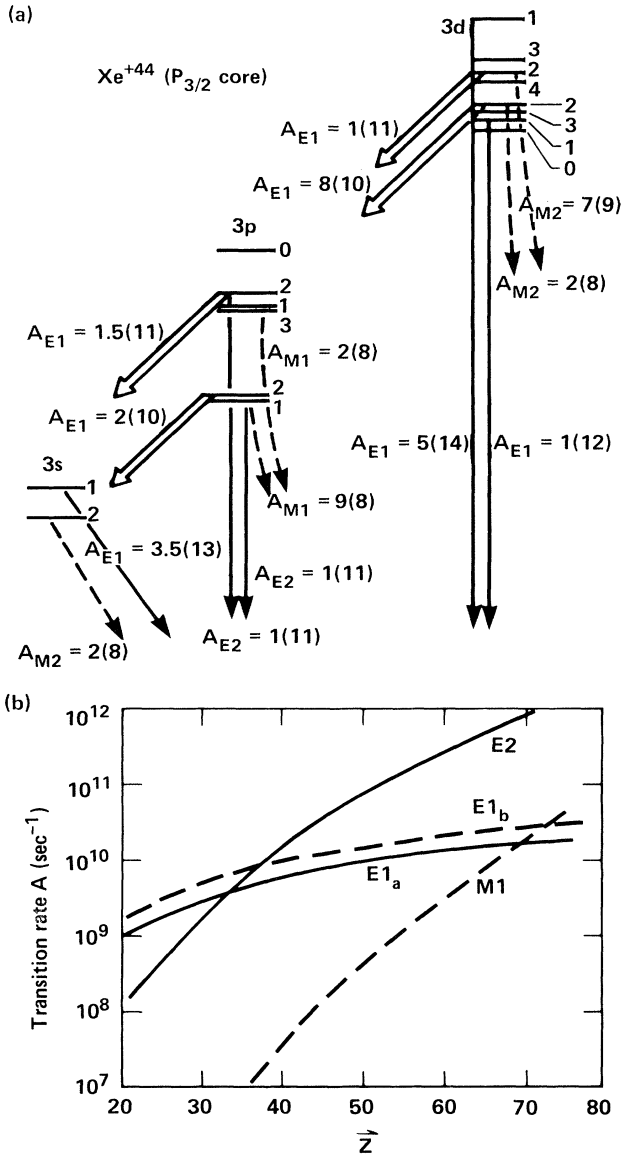

FIG. 1. (a) Grotrian diagram for the $1s^22s^22p^53s$, $3p$, and $3d$ configurations with the $J=\frac{3}{2}$ core for Xe^{44+}. Observed transitions are indicated with a solid line; 1(11) means 1×10^{11} sec^{-1}. (b) Scaling of selected transition rates with Z. All transitions involve the $1s^22s^22p^5(J=\frac{3}{2})$ core; the $E2$ and $M1$ transitions shown connect the $3p_{1/2}(J=2)$ and $3p_{1/2}(J=1)$ levels, respectively, with the $1s^22s^22p^6\,{}^1S_0$ ground state. The two $E1$ transitions have the common $3s_{1/2}(J=2)$ lower level and connect to the same upper levels as the $E2$ ($E1$a, solid line) and $M1$ ($E1$b, dashed line). The $M1$ rate should be large enough for observation with our technique at approximately $Z=75$.

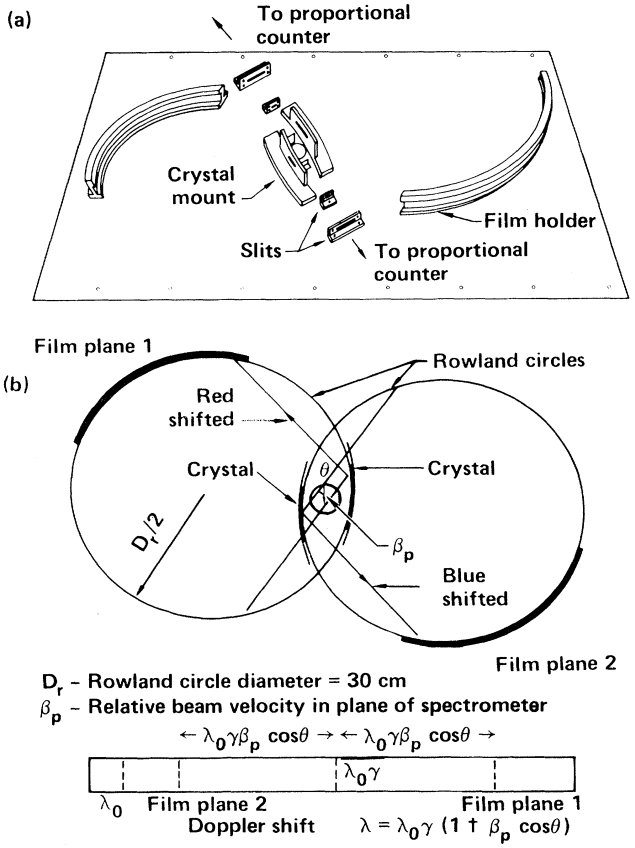

FIG. 2. (a) The dual Johann spectrometer and its components. The ion beam passes out of the plane of the paper between the crystal holders. (b) A schematic showing how the spectral lines from a crystal pair are averaged to remove the linear Doppler shift.

$^{132}Xe^{+30}$ are obtained from the Lawrence Berkeley Laboratory SuperHILAC with an energy of 8.5 MeV/u ($v=0.0134c$). The beam passes through a thick carbon foil ($\approx 600\ \mu g/cm^2$) to establish charge-state equilibrium. It then passes through a thin exciter foil ($\approx 50\ \mu g/cm^2$) located in the dispersive plane of our dual Johann crystal spectrometer. The beam is then collected in a Faraday cup and monitored to normalize the exposures. We pay particular attention to the beam tune at the beginning of the experiment as any unnecessary divergence adds to the linewidths. The tune is then monitored during the run by beam profile monitors. The beam can also be magnetically analyzed to determine the percentage of the beam in a particular charge state.

The design of the dual Johann spectrometer shown in Fig. 2 allows us to obtain wide wavelength coverage ($\theta_b=27°$–$68°$) with spectral resolution of $\lambda/\Delta\lambda=1500$ full width of half maximum (FWHM) while simultaneously measuring both the beam velocity and the linear Doppler angle. The Doppler angle is extracted by an averaging of the results in the two coplanar spectrometers with respect to lines from a standard x-ray calibration source, while the beam velocity is obtained

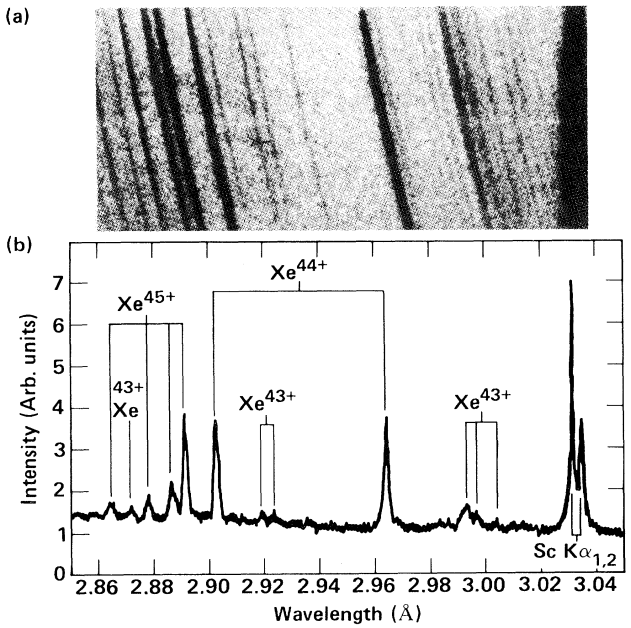

FIG. 3. (a) Raw data taken with 8 mC of charge. The straight lines are from the calibration source and the slanted ones are from the Xe beam. (b) Digitized data showing the calibration lines and several Xe^{45+} and Xe^{44+} lines. Both spectra represent about one-fifth of the total wavelength range covered.

from the slope of the lines emitted by the moving ions measured with respect to the slope of the lines emitted by the stationary source. The diffracted photons are recorded on Kodak DEF or No-screen film which is then digitized with a Perkin Elmer PDS densitometer.

A sample spectrum is shown in Fig. 3. The vertical lines are from the calibration source and the slanted ones are from the moving ions. The slant is caused by the Doppler shift of the radiation as the angle between the emitted light and the ion beam velocity changes along the film plane in a direction perpendicular to the dispersive plane.

Shown in Table I are several $\Delta n = 0$ energy intervals in F- and Ne-like xenon. The theoretical results were obtained with use of a relativistic Hartree-Fock calculation done by Scofield and a calculation done by Chen using the code of Grant.[13] The experimental results are obtained by taking the difference between the energies of two $\Delta n = 1$ x-ray transitions connecting both of the levels indicated with a common third level. For example, the first entry in Table I was obtained by subtracting the measured energies of the two features labeled Xe^{44+} in Fig. 3(b). The last entry is the only entry not requiring the observation of an electric quadrupole transition. It is included in this article because of its unique theoretical interest.[6] In all, 24 Ne-like and over 140 F-like transitions were considered in addition to the strongest O-like and Na-like transitions in making the identifications used in this analysis. The uncertainty in our measurements is estimated at 2×10^{-3} Å (absolute wavelengths) and 2.5×10^{-4} Å (relative wavelengths) at three standard deviations including systematic effects and has been increased when necessary to account for blending of lines. The uncertainty in the absolute wavelength is dominanted by potential systematic effects (i.e., uncertainty between crystallographic and optical surfaces on our diffraction crystals) and can be substantially improved, while the uncertainty in the relative wavelength is determined by line shapes and statistics. Note that many of the uncertainties quoted are better than those given for the $2p$-$2s$ Be-like krypton transition[24] (169.9 Å $\pm 0.3\%$) obtained by a direct measurement of the $\Delta n = 0$ extreme-ultraviolet radiation with the same beam-foil light source. The present technique can also easily be extended to much higher Z with existing accelerators and technologies. The requirement to move only a few units in nuclear charge so as to maintain contact with isoelectronic squences is not a necessity with the current technique.

This result represents the first direct observation of $E2$ transitions with rates comparable to the allowed $E1$ rates. The existence of this radiation allows investigation of atomic structure, without the requirement of a connection to the existing isoelectronic extrapolations, in a regime where relativistic effects dominate and quantum electrodynamic effects cannot be ignored. The method also gives access to energy-level differences in the 30–150-Å region where high-resolution spectroscopy can currently be done only at an extreme sacrifice in sensitivity. Also, this technique should be valuable for investigating the role of nuclear effects on the lifetimes of metastable levels by resolving transitions induced by hyperfine quenching. The presence of $M1$ rates [see Fig. 1(b)], large enough for observation with our technique at readily attainable nuclear charges ($Z = 70$'s), will yield even more information about the physics of highly ionized atoms.

The authors are grateful to Dr. Mark Eckart for help in the initial design of the experiment. We would also like to thank Roger Morales and Steven Smith for expert help in the construction and installation of the experiment and the technical staff of the SuperHILAC for their assistance during the course of the experiment. This work was performed under the auspices of the U. S. Department of Energy by Lawrence Livermore National Laboratory under Contract No. W-7405-Eng-48.

[a]Present address: KMS Fusion, Inc., Ann Arbor, Mich. 48106.

[1]D. L. Matthews *et al.*, Phys. Rev. Lett. **54**, 110 (1985); M. D. Rosen *et al.*, Phys. Rev. Lett. **54**, 106 (1985).

[2]C. Jupen and Ulf Litzen, Phys. Scr. **30**, 112 (1984).

[3]E. Träbert, Z. Phys. A **319**, 25 (1984).

TABLE I. Comparison of selected $\Delta n = 0$ intervals in Xe^{45+} and Xe^{44+} (F- and Ne-like) with theory. Levels are designated by (hole state, excited electron); for example, $((P_{1/2}P_{3/2})_1, S_{1/2})_{3/2}$ means that the $1s^2 2s^2 2p^4$ core is missing one $p_{1/2}$ and one $p_{3/2}$ electron coupled to angular momentum 1, which is coupled to the $3s_{1/2}$ excited electron to give a total angular momentum of $J = \frac{3}{2}$.

Interval	exp(±0.5 eV)	theory[a] Scofield	theory[a] Chen
Xe^{44+}			
$1s^2 2s^2 2p^5 3p - 1s^2 2s^2 2p^5 3s$			
$(P_{3/2}, P_{1/2})_2 - (P_{3/2}, S_{1/2})_1$	89.1	89.6	89.8
$(P_{3/2}, P_{3/2})_2 - (P_{3/2}, S_{1/2})_1$	182.9	183.2	183.5
$(P_{1/2}, P_{3/2})_2 - (P_{1/2}, S_{1/2})_1$	186.5±1eV	184.2	184.5
$1s^2 2s^2 2p^5 3d - 1s^2 2s^2 2p^5 3p$			
$(P_{3/2}, d_{3/2})_1 - (P_{3/2}, P_{1/2})_2$	196.5	198.1	198.1
$(P_{3/2}, d_{5/2})_1 - (P_{3/2}, P_{3/2})_2$	157.2	160.2	160.3
$(P_{1/2}, d_{3/2})_1 - (P_{1/2}, P_{3/2})_2$	31.3±1eV	130.0	130.0
Xe^{45+}			
$1s^2 2s^2 2p^4 3p - 1s^2 2s^2 2p^4 3s$			
$((P_{3/2})^2_0, P_{1/2})_{1/2} - ((P_{3/2})^2_0, S_{1/2})_{1/2}$	81.6	83.2	83.3
$((P_{3/2})^2_2, P_{3/2})_{3/2} - ((P_{3/2})^2_2, S_{1/2})_{3/2}$	200.0	201.1	201.6
$((P_{1/2}P_{3/2})_2, P_{1/2})_{5/2} - ((P_{1/2}P_{3/2})_2, S_{1/2})_{3/2}$	79.5	79.8	80.3
$((P_{1/2}P_{3/2})_2, P_{3/2})_{5/2} - ((P_{1/2}P_{3/2})_2, S_{1/2})_{3/2}$	175.7	178.1	178.0
$1s^2 2s^2 2p^4 3d - 1s^2 2s^2 2p^4 3p$			
$((P_{3/2})^2_0, d_{3/2})_{3/2} - ((P_{3/2})^2_0, P_{1/2})_{1/2}$	190.8	187.6	187.9
$((P_{3/2})^2_2, d_{5/2})_{5/2} - ((P_{3/2})^2_2, P_{3/2})_{3/2}$	116.7	115.9	115.9
$1s^2 2s 2p^6 (S_{1/2}) - 1s^2 2s^2 2p^5 (P_{3/2})$	641.8±3eV	642.1	641.7
$1s^2 2s^2 2p^5 (P_{1/2}) - 1s^2 2s^2 2p^5 (P_{3/2})$	334.9±3eV	334.5	334.8

[a]Reference 12.

[4]C. Jupen, Mon. Not. Roy. Astron. Soc. **208**, 1 (1984).

[5]J. Reader, Phys. Rev. A **26**, 501 (1982).

[6]P. G. Burkhalter, J. Reader, and R. D. Cowan, J. Opt. Soc. Am. **67**, 1521 (1977); M. W. D. Mansfield *et al.*, J. Phys. B **11**, 1521 (1978).

[7]K.-N. Huang, Y. K. Kim, T. Cheng, and J. P. Desclaux, Phys. Rev. Lett. **48**, 1245 (1982).

[8]B. Edlén, Phys. Scr. **28**, 51 (1983).

[9]L. N. Ivanov and E. P. Ivanova, At. Data Nucl. Data Tables **24**, 96 (1979).

[10]I. P. Grant *et al.*, Comput. Phys. Commun. **21**, 207 (1980).

[11]J. P. Desclaux, Comput. Phys. Commun. **9**, 31 (1975).

[12]R. D. Cowan, *The Theory of Atomic Structure and Spectra* (Univ. of California Press, Berkeley, 1981).

[13]J. H. Scofield and M. Chen, private communication.

[14]R. Marrus, in *Cargese Lectures in Physics,* edited by M. Levy (Gordon and Breach, London, England, 1977).

[15]I. S. Bowen, Nature (London) 120 (1927), and Astrophys. J. **67**, 1 (1928).

[16]K. T. Chen, Y. K. Kim, and J. P. Desclaux, At. Data Nucl. Data Tables **24**, 111 (1979).

[17]B. Denne, E. Hinnov, S. Suckewer, and S. Cohen, Phys. Rev. A **28**, 206 (1983).

[18]G. H. Shortley, Phys. Rev. **57**, 225 (1940).

[19]T. Gil and J. Held, Z. Phys. A **312**, 343 (1983).

[20]D. R. Wood and K. L. Andrew, J. Opt. Soc. Am. **58**, 343 (1968).

[21]Y. Couturie, B. Yaakobi, U. Feldman, and G. A. Doschek, J. Opt. Soc. Am. **71**, 1309 (1981).

[22]H. G. Berry, J. Desesquelles, K. T. Cheng, and R. M. Schectman, Phys. Rev. A **18**, 546 (1978).

[23]C. J. Hailey, R. E. Stewart, G. C. Chandler, D. D. Dietrich, and R. J. Fortner (to be published).

[24]D. D. Dietrich, J. A. Leavitt, H. Gould, and R. Marrus, Phys. Rev. A **22**, 1109 (1980).

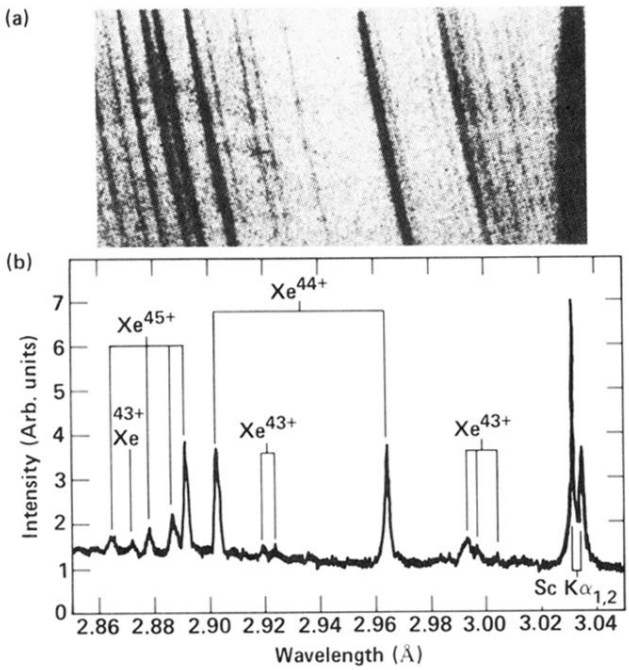

FIG. 3. (a) Raw data taken with 8 mC of charge. The straight lines are from the calibration source and the slanted ones are from the Xe beam. (b) Digitized data showing the calibration lines and several Xe^{45+} and Xe^{44+} lines. Both spectra represent about one-fifth of the total wavelength range covered.